Gait Event Prediction of People with Cerebral Palsy using Feature Uncertainty: A Low-Cost Approach

Saikat Chakraborty
School of Computer Engineering, Kalinga Institute of Industrial Technology (KIIT), India; Machine Intelligence and Bio-motion Research Lab., Department of Computer Science and Engineering, National Institute of Technology Rourkela
India
saikat.chakrabortyfcs@kiit.ac.in

Noble Thomas
Machine Intelligence and Bio-motion Research Lab., Department of Computer Science and Engineering, National Institute of Technology
Rourkela, India
mailmenoble30@gmail.com

Anup Nandy
Machine Intelligence and Bio-motion Research Lab., Department of Computer Science and Engineering, National Institute of Technology
Rourkela, India
nandy.anup@gmail.com

ABSTRACT

Incorporation of feature uncertainty during model construction explores the real generalization ability of that model. But this factor has been avoided often during automatic gait event detection for Cerebral Palsy patients. Again, the prevailing vision-based gait event detection systems are expensive due to incorporation of high-end motion tracking cameras. This study proposes a low-cost gait event detection system for heel strike and toe-off events. A state-space model was constructed where the temporal evolution of gait signal was devised by quantifying feature uncertainty. The model was trained using Cardiff classifier. Ankle velocity was taken as the input feature. The frame associated with state transition was marked as a gait event. The model was tested on 15 Cerebral Palsy patients and 15 normal subjects. Data acquisition was performed using low-cost Kinect cameras. The model identified gait events on an average of 2 frame error. All events were predicted before the actual occurrence. Error for toe-off was $\approx$ 21% less than the heel strike. Incorporation of the uncertainty factor in the detection of gait events exhibited a competing performance with respect to state-of-the-art.

KEYWORDS

Cerebral Palsy; Dempster-Shafer theory; gait event; gait phase; Kinect v2

ACM Reference Format:
Saikat Chakraborty, Noble Thomas, and Anup Nandy. 2023. Gait Event Prediction of People with Cerebral Palsy using Feature Uncertainty: A Low-Cost Approach. In *INTERNATIONAL CONFERENCE ON MULTIMODAL INTERACTION (ICMI '23), October 09–13, 2023, Paris, France.* ACM, New York, NY, USA, 6 pages. https://doi.org/10.1145/3577190.3614125

ICMI '23, October 09–13, 2023, Paris, France

ACM ISBN 979-8-4007-0055-2/23/10…$15.00
https://doi.org/10.1145/3577190.3614125

1 INTRODUCTION

Cerebral Palsy (CP) refers to a set of movement and postural disorders caused by non-progressive injury in fetal or infant brain [15]. As per a recent report [19], more than 4 per 1000 children across the world suffer from CP. In developing countries, the number of CP patients is alarming. Accurate clinical intervention and rehabilitation treatment using gait analysis has become a vital issue for this population [9]. Annotation of gait events, especially heel strike (HS) and toe-off (TO), is a crucial preprocessing step to perform these analyses [12].

Generally, the manual labeling technique is followed in clinics to annotate the events, which is laborious and time-consuming too [12]. For pathological gait, like CP, manual annotation becomes more challenging for their atypical gait pattern. Again, the force plate, which is considered as the "gold standard" for gait event detection, has been reported to be not suitable in case of CP population [3, 12].

Recently, some automated gait event detection algorithms based on computational intelligence techniques have been proposed [3, 10, 12, 16]. Miller *et al.* [12]used a sliding window to feed a neural network on an incremental basis and used that model to compute gait events. Each variable within the window was converted to a standard form that resulted in a feature vector of size 315. The proposed model exhibited a competing performance, but the authors did not validate this method quantitatively against the normal subjects, which limits its versatility. Kidzińsk *et al.* [10] proposed a Long ShortTerm Memory (LSTM) for event detection (HS and TO) in both normal and pathological populations. Lower limb body positions and joint kinematics were used as the input vector corresponding to each frame. The network consists of a multilayer LSTM where a fixed number of frames were used to provide the input. The network mapped the input to a n-dimensional time series. Local maxima on the output time series were marked as the gait events. But, the usage of a large-size feature vector increased the complexity of the system. Lempereur *et al.* [11] proposed a deep neural network named *DeepEvent* to detect two gait events. Heel, toe, and lateral malleolus markers positional and velocity data were fed to the model. A set of bidirectional LSTM units was used to construct the learning network, which also consisted of a dropout layer and a distributed dense layer. Gait events were encoded using one-hot encoding method. The study obtained a competing result with an expense of complex network.

It is noteworthy that almost all of the above mentioned studies used a set of salient features where event annotation was mapped to binary classification problem (i.e., HS and TO frames classification). But, all selected features may not equally support a specific classification decision [8]. Even some may not exhibit any evidence for the classification, which attributes uncertainty in decision making. Consideration of this uncertainty factor during feature analysis is essential in clinical decision-making [8]. It creates a significant impact on model performance and demonstrates a real estimation of the model capacity [20]. Although exhibiting a competing performance, the above-mentioned studies have ignored this crucial issue while detecting gait events.

Another vital fact is that most of the vision-based systems for CP gait event detection have used expensive sensors (e.g., Vicon, etc.), which made the overall system cost high. These systems are not affordable for many clinics, especially in developing countries. A low-cost solution for this issue is an urgent need.

This study proposes a state-space model, in a low-cost environment, by exploring the temporal evolution of gait signal. Dempster-Shafer theory of evidence (DST) [6, 17] was used to quantify feature uncertainty. Signal segmentation between two consecutive states was mapped to a binary classification problem. Gait velocity of both ankle joints was given as the input feature to the model. The 4-state model annotates gait events for both limbs individually. Gait phases were also estimated following the detection of events. The contributions of this study are summarized as:

- Construction of a low-cost system for data acquisition on overground.
- Detection of gait event and phase for CP patients using the aforementioned architecture.
- Proposing a state-space model where feature uncertainty was quantified to allocate frames to a state. Gait events were detected by identifying the state transition frames.

The rest of the paper is divided into the following parts: section 2 describes the study populations, the architecture of the data acquisition system, construction of the proposed model, and data analysis. Model outputs and corresponding discussions are elaborated in sections 3 and 4, respectively. Finally, the study concluded by providing some future research directions in section 5.

2 METHODS

2.1 Population

Fifteen children and adolescent with CP (CAwCP) (age (years): 12.55 ± 2.13, height (cm): 130.15 ± 14.87, gender(M/F): 8/7, GMFCS levels: I and II) with having no other diseases or surgical history which can affect their gait were recruited from the Indian Institute of Cerebral Palsy (IICP), Kolkata. CP types were: Diplegic (5), Hemiplegic (right side) (5), Hemiplegic (left side) (3), and Athetoid (2). Along with that, 15 typically developed children and adolescent (TDCA) (age (years): 12.45 ± 3.51, height (cm): 132.06 ± 14.09, gender(M/F): 9/6) were recruited from REC School, NIT Rourkela, Odisha. Approval to conduct this research was taken from the competent authority. Informed consent was taken from the subjects or their guardians for conducting the experiment.

2.2 Experimental setup

A set of Kinect v2 sensors were used for data acquisition. Due to the limited field of view (FoV), a single sensor can not track body joints for a long walking path (i.e., 10m or 8m) which is generally used in the clinical setting [7]. Hence, Inspired by the work of Geerse et al. [7], a 3-Kinect-based architecture was established for data acquisition (see figure 1). Client-server protocol was used to control the sensors. Kinects v2, having horizontal FoV 70°, were placed at 35° angle with the walking path on tripods at 0.8m height. Tilt angle of the Kinects was 0°. The common tracking volumes for the successive Kinects was set to $\approx 0.5m$ which was empirically tested to be acceptable for the next Kinect to recognize the human skeleton. Each Kinect was connected to separate computers which were controlled by a server. Greyware's DomainTime II (Greyware Automation Products, Inc.) was used to synchronize the clocks of the computers. Participants were asked to walk at self-selected speed (barefoot) from 4m distance of the 1st Kinect. Data (skeletal data stream) were started to collect after 1m walking. The walking path length was 12m, out of which the effective length of data acquisition was 10m. For each subject, 5 consecutive trials were taken. The approximate sampling rate of the system was 30 Hz. We have followed the protocol described in [7, 14] to preprocess and combine the time series data collected from the three Kinects.

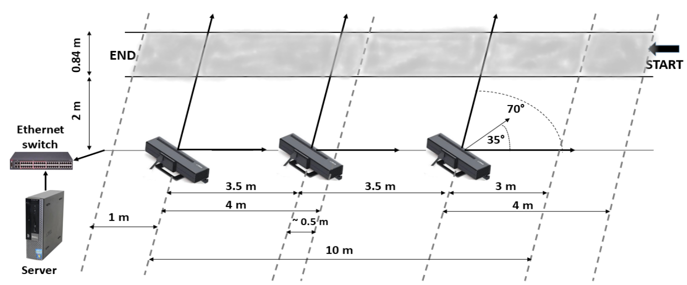

Figure 1: Data acquisition system

2.3 Model Construction

Considering the variety of CP types, this study estimated gait events individually for each limb. Gait cycle was segmented into 4 phases; first double limb support (FDLS), single limb support for the left limb (LSL), second double limb support (SDLS), and single limb support for the right limb (RSL). Phase FDLS was marked when the left foot is in the forward position. Hence, the sequence of phases should be: FDLS -> LSL -> SDLS -> RSL. We assumed that the above temporal sequence would be true for both populations. Based on the above assumption, a hypothetical model was constructed (see figure 2). Each state in the model corresponds to individual phases. In subsequent discussions, state and phase have been used interchangeably.

+

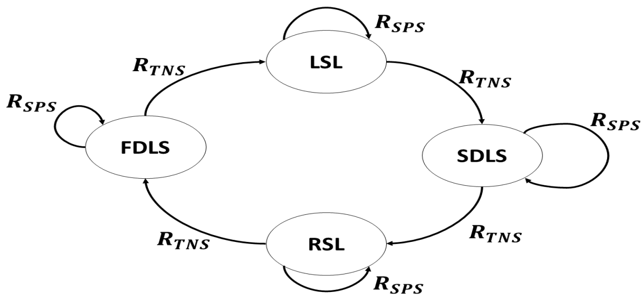

Figure 2: Hypothetical model

The movement of gait signal across the phases was modeled by quantifying the underlying uncertainty of input features. Velocity was reported as one of the most important features for CAwCP [4]. Hence, the velocity of both ankles (anterior-posterior (A-P) and vertical (V) directions) was taken as input. DST used these features as the source of evidences to construct a classifier, often termed as *Cardiff Classifier* [2], which allocated frames between two consecutive states. In-sample group (i.e., training set) was formed using 11 TDCA and 10 CAwCP, while the remaining subjects were used for the out-of-sample group (i.e., test set). During construction of the classifier, the elementary hypotheses for frame allocation were defined as: { present state (PS), next state (NS) }. So, the hypothesis space became: $\{\{\emptyset\}, \{PS\}, \{NS\}, \{PS, NS\}\}$. Using the Kolmogorov-Smirnov test, the Fréchet distribution was found to fit the best for the input features, and thus, it was used to convert the input features into confidence factor. Inspired by the work of Jones et al. [8], expert knowledge was used to set the control parameters for the in-sample group. Dempster's rule of combination [6, 17] was used to construct the final body of evidence (τ) from each source of evidence (i.e., each input feature). The decision on frame allocation between two consecutive phases was guided by τ. The free movement of probability mass across the hypothesis space, specifically to the subset $\{PS, NS\}$, quantify and associates feature uncertainty in decision making [8]. The model learned the control parameters from the in-sample group to classify the frames in the out-sample group.

Since a gait cycle could start from any one of the 4 phases, for the initial frame, τ corresponding to all four states were computed. The phase having the highest value for τ was marked as the initial phase. The frame allocation rules between two consecutive phases are stated below:

- R_{SPS}: if $\tau(\{PS\}) > \tau(\{NS\}) + \tau(\{PS, NS\})$, OR if $\tau(\{PS\}) > \tau(\{NS\})$ but $\tau(\{PS\}) < \tau(\{NS\}) + \tau(\{PS, NS\})$, then the corresponding frame will stay at present phase;
- R_{TNS}: if $\tau(\{NS\}) > \tau(\{PS\})$ but $\tau(\{NS\}) < \tau(\{PS\}) + \tau(\{PS, NS\})$, then the corresponding frame will transit to the immediate next phase.

2.4 Event detection

Events were detected for individual limbs by marking the transition frames. We have marked 4 events as:

- FDLS − > LSL = Right foot TO (RTO)
- LSL − > SDLS = Right foot HS (RHS)
- SDLS − > RSL = Left foot TO (LTO)
- RSL − > FDLS = Left foot HS (LHS)

Right foot toe-off was identified by the last frame of first double limb support, whereas, the right foot heel strike was marked by the first frame of second double limb support. Similar, strategy was adopted for the other the limb also. Following Xu et al. [21], we have approximated HS and TO from the ankle data. Like [1, 10, 18], ground truth (GT) was generated by manual annotation with an expert. Kinect skeleton video (≈ 30 Hz) and a stopwatch were used during the annotation.

2.5 Data analysis

The detected gait events and phases were evaluated on the basis of mean relative difference (MRD) and mean absolute difference (MAD) [13], which were computed using the time difference between GT and model prediction. For gait event, relative difference E_{RD} was computed as:

$$E_{RD} = t_{GT} - t_{model} \quad (1)$$

In equation 1, t_{model} and t_{GT} are event detection time (ms) for the proposed model and GT, respectively. A positive value indicates that the model predicts the event before the actual occurrence, whereas a negative value indicates that the prediction was after the actual occurrence. The absolute value of E_{RD}, i.e., E_{AD} (equation 2) refers the magnitude of error.

$$E_{AD} = |t_{GT} - t_{model}| \quad (2)$$

Phase duration (PD) was estimated using the detected events. The same metrics were used for evaluation of the PD. In this case, the relative difference (P_{RD}) and absolute difference (P_{AD}) were computed as:

$$P_{RD} = PD_{GT} - PD_{model} \quad (3)$$

$$P_{AD} = |PD_{GT} - PD_{model}| \quad (4)$$

In equations 3 and 4, PD_{GT} and PD_{model} refer to phase duration for GT and the proposed model respectively. A positive value means that the estimated value for PD (by the model) is less than the GT, whereas a negative value indicates that the estimated value for PD (by the model) is higher than the GT. In addition, the distribution of errors (in the case of P_{RD}) for the 4 phases was also assessed.

3 RESULTS

Figure 3 demonstrates the allocation of frames to consecutive phases. The transition frames (marked by red dot), used to detect gait events, fall in the uncertainty zone of the simplex plot. For the subsequent frames, the uncertainty value decreases. The transition frames associate the highest uncertainty value. As the signal travels through the states, the frames keeps on moving (in time line) from the deterministic zone to the uncertainty zone. For example, when the state transits from FDLS to LSL, the corresponding frame (marked by red dot) moves to the uncertainty zone of LSL (see Figure 3(a)). The green crosses represent the previous frames of the transition frame. All the green labeled frames are situated in the deterministic zone of FDLS state. Similarly, during the transition from LSL to SDLS (Figure 3(b)) the transition frame falls in the uncertainty zone of

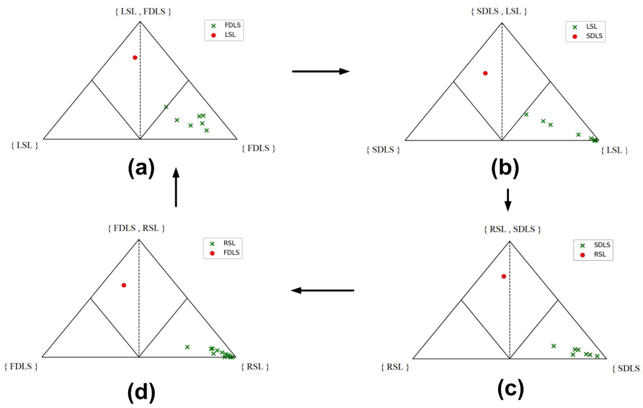

Figure 3: Simplex plots showing the allocation of frames throughout a gait cycle (subj #1 CAwCP). (a) FDLS to LSL, (b) LSL to SDLS, (c) SDLS to RSL, (d) RSL to FDLS.

SDLS and all its previous frames are situated in the deterministic zone of LSL. Similar phenomenon keeps on happening for all the subsequent transition periods and cycle to cycle. Note that when a frame is in the uncertainty zone of the present state, it can not be termed as a transition frame.

Table 1 demonstrates the evaluation metrics for the gait events and corresponding phases. The proposed model was evaluated for both normal and pathological (i.e., CAwCP) populations. For gait events, on average, the model prediction error (i.e., absolute frame difference) was approximately 2 frames (considering the average frequency of Kinect 30 Hz and average MADs for CAwCP and TDCA, i.e., 92.78 ms (≈ 3 frames) and 67.84 ms (≈ 2 frames) respectively). It can be seen that all the events were predicted by the model before the actual occurrence. Figures 4 and 5 exhibit the frequency distributions of E_{RD} for all predicted gait events for CAwCP and TDCA, respectively. In the case of CAwCP (see figure 4), the model performed the best for RTO and LTO, where on average, 46% of frames encountered 0 frame error. In the case of TDCA (see figure 5), LTO exhibits the best result with 57% of 0 frame error, whereas moderate results were observed for the other events.

The estimated PDs were higher than GT for double limb supports (CAwCP) and single limb supports (TDCA) (see table1). In the case of CAwCP, the distribution of P_{RD} demonstrates comparatively low error and variance for the double limb support phases (see figure 6(a)), whereas, for TDCA, the variance is comparatively low for FDLS (see figure 6(b)). It is to be noted that the higher magnitude of time difference is due to the low frequency of Kinect, which was not altered to keep originality of data pattern. Hence, when comparing the proposed model, more emphasis might be given to the frame error than the time difference.

4 DISCUSSION

This study proposes an automatic gait event detection model for TDCA and CAwCP patients using a low-cost system setup. It carries a multifaceted clinical significance. First, the proposed model determines gait events separately for each limb which could facilitate

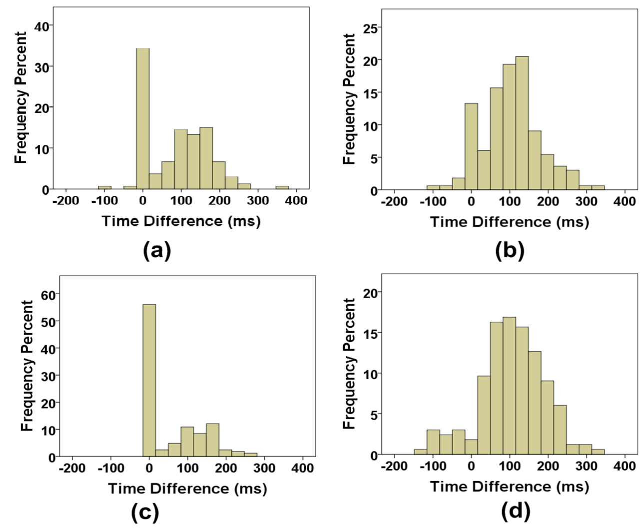

Figure 4: Frequency distribution of RD (for CAwCP). (a) RTO, (b) RHS, (c) LTO, and (d) LHS.

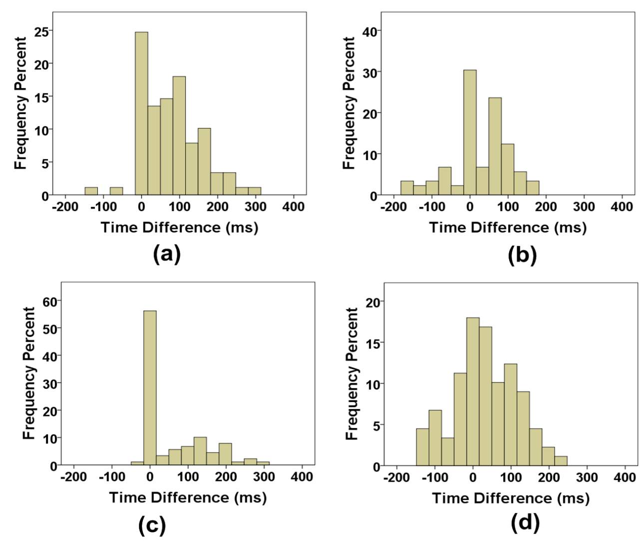

Figure 5: Frequency distribution of RD (for TDCA). (a) RTO, (b) RHS, (c) LTO, and (d) LHS.

the diagnosis of gait abnormality individually for each limb. Second, for pathological gait, detection of gait events using force plate encounters a serious problem [12]. Patients often fail to place their foot properly on the force plate, which consequences unreliability for the acquired data. The proposed automated system presents a solution to this problem. The unobtrusiveness of the acquisition system makes it more subject-friendly. Third, the model was build based on a single feature, i.e., ankle velocity, which can be easily extracted from gait signal. This simplicity could make it attractive for the clinical staff. Fourth, consideration of uncertainty during model building improves the likelihood of interpretability of results which is vital for clinical decision making [5]. Finally, this study

Table 1: Relative and absolute errors for different events and phases. Data were represented in mean ± 1 standard deviation form

Evaluation Metric	Population	Events (mean ± standard deviation)				Phases (mean ± standard deviation)			
		RTO	RHS	LTO	LHS	FDLS	LSL	SDLS	RSL
MRD (ms)	CAwCP	86.87 ± 80.69	102.57 ± 74.76	56.85 ± 73.83	106.35 ± 84.74	-16.23 ± 83.17	44.03 ± 12.30	-48.39 ± 69.13	20.06 ± 26.57
	TDCA	77.62 ± 76.92	25.24 ± 74.63	59.81 ± 82.33	32.17 ± 82.46	51.55 ± 81.22	-33.17 ± 11.27	26.13 ± 78.36	-45.39 ± 17.39
MAD (ms)	CAwCP	88.46 ± 78.95	105.75 ± 70.19	57.84 ± 73.82	119.07 ± 65.68	69.32 ± 49.77	115.36 ± 67.21	71.34 ± 44.67	103.51 ± 75.68
	TDCA	81.94 ± 71.36	60.06 ± 50.58	60.04 ± 81.06	69.33 ± 54.87	73.53 ± 62.88	103.37 ± 60.91	62.77 ± 53.33	91.36 ± 6.39

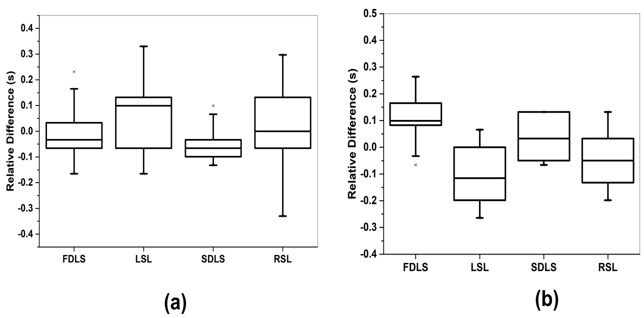

Figure 6: Distribution of relative errors for each phases. (a) CAwCP, (b) TDCA

proposes an affordable gait event detection system, especially for the CAwCP population, which is an urgent clinical need.

The proposed model was compared with the work of Kidzińsk et al. [10] and Salazar et al. [16], where CP patients were treated as one of the main pathological populations. All of them used expensive cameras having high sampling frequency (i.e., 120 Hz). Kidzińsk et al. [10] reported ≈ 2.20 (18.3 ms) and ≈ 1.50 (12.5 ms) frame errors (averaged over all subjects) for HS and TO events, respectively. Salazar et al. [16] reported ≈ 1.92 (15.95 ms) and ≈ 4.25 (35.45 ms) frame errors (averaged over all subjects) for HS and TO events, respectively. In the case of HS event, the proposed method closely resembles [10] with ≈ 2.65 (88.55 ms) frame error (averaged over all subjects), while for TO even, it performs better than [16] with ≈ 2.15 (72.07 ms) frame error which is also close to [10]. Compared to [10, 12], where a multi-dimensional feature vector was used for training, our model uses only a single feature. Moreover, on the issue of affordability, the proposed system beats the others (i.e., [10, 16]).

The model demonstrated comparatively low error (on average) for the normal subjects (2.03 frame error (TDCA) vs 2.78 frame error (CAwCP)). This might be due to the atypical gait pattern of CAwCP patients, which caused some incorrect state transitions for some subjects. In the case of CAwCP, frame error for the TO event was 34% less than the HS. Specifically, LTO was detected 35% more accurately than RTO (see table 1). This might be due to the left alignment of sensors with respect to the walking path, which allowed the system to track the left ankle more accurately than its counterpart. It is observable from table 1 that the magnitude of error is comparatively high for single limb support time (for both populations). This might be due to overall 18% higher detection error for HS events than TO. Figures 4 and 5 also confirm the results of table 1. Higher magnitude of frequencies for time differences was observed in HS events compared to TO events, especially for the CAwCP group.

This study proposes a gait event detection model dedicatedly for CP patients. However, it was tested for normal population also. Although providing a competing performance, the system comes up with some limitations. The placing of Kinects only on a single side of the walking track introduced a partial self-occlusion problem which might impact the model performance to some extent. Placement of Kinects on both sides of the track could be a solution to this problem. But, it requires more cameras which will account for more expenditure. Again, the low frequency of Kinect introduced a comparatively high magnitude of time difference. Up sampling could be a solution, but it could alter the original gait pattern. Approximation of HS and TO from the ankle data could impact the results. But, that process was necessary to avoid the noisy foot marker data [21]. Moreover, due to unavailability constraints, adult CP subjects were not included in this study, and experimental sample size was not so large also.

5 CONCLUSION

This study proposes a low-cost solution for automated gait event detection and phase estimation considering the feature uncertainty embedded in gait signal. The model demonstrated a competing performance for both CAwCP and TDCA populations. In future, this model could be tested for some other pathological populations to prove its versatility. Again, some other arrangement of Kinect which could reduce the self-occlusion problem can be investigated with this model.

REFERENCES

[1] Alberto Alvarez-Alvarez, Gracian Trivino, and Oscar Cordon. 2011. Human gait modeling using a genetic fuzzy finite state machine. *IEEE Transactions on Fuzzy Systems* 20, 2 (2011), 205–223.
[2] PR Biggs, GM Whatling, C Wilson, and CA Holt. 2019. Correlations between patient-perceived outcome and objectively-measured biomechanical change following Total Knee Replacement. *Gait & posture* 70 (2019), 65–70.
[3] Dustin A Bruening and Sarah Trager Ridge. 2014. Automated event detection algorithms in pathological gait. *Gait & posture* 39, 1 (2014), 472–477.
[4] Saikat Chakraborty, Anup Nandy, and Trisha M Kesar. 2020. Gait deficits and dynamic stability in children and adolescents with cerebral palsy: A systematic review and meta-analysis. *Clinical Biomechanics* 71 (2020), 11–23.
[5] National Research Council et al. 2006. *Completing the forecast: Characterizing and communicating uncertainty for better decisions using weather and climate forecasts.* National Academies Press.
[6] Arthur P Dempster. 1968. A generalization of Bayesian inference. *Journal of the Royal Statistical Society: Series B (Methodological)* 30, 2 (1968), 205–232.
[7] Daphne J Geerse, Bert H Coolen, and Melvyn Roerdink. 2015. Kinematic validation of a multi-Kinect v2 instrumented 10-meter walkway for quantitative gait assessments. *PloS one* 10, 10 (2015), e0139913.

[8] Lianne Jones, Malcolm J Beynon, Catherine A Holt, and Stuart Roy. 2006. An application of the Dempster–Shafer theory of evidence to the classification of knee function and detection of improvement due to total knee replacement surgery. *Journal of biomechanics* 39, 13 (2006), 2512–2520.

[9] Joarder Kamruzzaman and Rezaul K Begg. 2006. Support vector machines and other pattern recognition approaches to the diagnosis of cerebral palsy gait. *IEEE Transactions on Biomedical Engineering* 53, 12 (2006), 2479–2490.

[10] Łukasz Kidziński, Scott Delp, and Michael Schwartz. 2019. Automatic real-time gait event detection in children using deep neural networks. *PloS one* 14, 1 (2019), e0211466.

[11] Mathieu Lempereur, François Rousseau, Olivier Rémy-Néris, Christelle Pons, Laetitia Houx, Gwenolé Quellec, and Sylvain Brochard. 2020. A new deep learning-based method for the detection of gait events in children with gait disorders: Proof-of-concept and concurrent validity. *Journal of biomechanics* 98 (2020), 109490.

[12] Adam Miller. 2009. Gait event detection using a multilayer neural network. *Gait & posture* 29, 4 (2009), 542–545.

[13] Shiwei Mo and Daniel HK Chow. 2018. Accuracy of three methods in gait event detection during overground running. *Gait & posture* 59 (2018), 93–98.

[14] Björn Müller, Winfried Ilg, Martin A Giese, and Nicolas Ludolph. 2017. Validation of enhanced kinect sensor based motion capturing for gait assessment. *PloS one* 12, 4 (2017), e0175813.

[15] Carol L Richards and Francine Malouin. 2013. Cerebral palsy: definition, assessment and rehabilitation. In *Handbook of clinical neurology*. Vol. 111. Elsevier, 183–195.

[16] José-de-Jesús Salazar-Torres. 2006. Validity of an automated gait event detection algorithm in children with cerebral palsy and non-impaired children. *Gait & Posture* 24 (2006), S130–S131.

[17] Glenn Shafer. 1976. *A mathematical theory of evidence*. Vol. 42. Princeton university press.

[18] Alexey Sharenkov, Alison N Agres, Julia F Funk, Georg N Duda, and Heide Boeth. 2014. Automatic initial contact detection during overground walking for clinical use. *Gait & posture* 40, 4 (2014), 730–734.

[19] Moshe Stavsky, Omer Mor, Salvatore Andrea Mastrolia, Shirley Greenbaum, Nandor Gabor Than, and Offer Erez. 2017. Cerebral palsy—trends in epidemiology and recent development in prenatal mechanisms of disease, treatment, and prevention. *Frontiers in pediatrics* 5 (2017), 21.

[20] Xizhao Wang and Junhai Zhai. 2016. *Learning with uncertainty*. CRC Press.

[21] Xu Xu, Raymond W McGorry, Li-Shan Chou, Jia-hua Lin, and Chien-chi Chang. 2015. Accuracy of the Microsoft Kinect™ for measuring gait parameters during treadmill walking. *Gait & posture* 42, 2 (2015), 145–151.